Supporting Information

A Pre-Steady State Kinetic Analysis of the αY60W mutant of *trans*-3-Chloroacrylic Acid Dehalogenase: Implications for the Mechanism of the Wild-type Enzyme[†]

Jamison P. Huddleston[‡], Gottfried K. Schroeder[‡], Kenneth A. Johnson[§,||], and Christian P. Whitman[‡,||,*]

Division of Medicinal Chemistry, College of Pharmacy, and the Department of Chemistry and Biochemistry, Institute for Cellular and Molecular Biology, University of Texas, Austin, TX 78712

Table S1. Summary of the Docking Study Results Using **9** and the Experimentally Determined K_m and k_{cat}

Enzyme	ΔG^a (kcal/mol)	ΔG^b (kcal/mol)	K_m (μM)	k_{cat} (s^{-1})
Wild-type	-4.8	-3.5	120 ± 10	2.5 ± 0.1
αY60W	-5.1	-3.6	70 ± 3.5	2.5 ± 0.1
αM7W	-4.8	-	120 ± 10	0.6 ± 0.1
αL57W	-4.0	-	N/A	N/A
βI37W	-4.8	-	>40,000	N/A
αF390W	-4.9	-	-	-
αF50W	-5.0	-	-	-

[a]The Δ*G* value for binding as predicted by AutoDock Vina for the binding of **9** to CaaD and mutants (Figure 2A).[1] [b]The Δ*G* for the binding of **9** to CaaD in which the αE52 points into the active site such that it can carry out the proposed chemistry (Figure 2C).

Table S2. Rates from the Conventional Analysis and Individual Fit by Simulation of the Binding of Bromide Ion and **4** to the αY60W Mutant of CaaD

Substrate	k_{on} (μM^{-1} s^{-1})	k_{off} (s^{-1})	K_d (μM)	F_0	ΔF	f/f_0 [a]
Bromide[b]	–	–	7400 ± 550	3.94 ± 0.01	0.56 ± 0.01	1.14 ± 0.02
	0.016 ± 0.002[c,d]	Fast[d]	12000[e] ± 250	3.95[f]	0.67 ± 0.12[c]	1.17 ± 0.03
4[b]	0.025 ± 0.001	28 ± 1.6	1120[g]/380[h]	4.52 ± 0.03	0.75 ± 0.02	1.16 ± 0.03
	0.028 ± 0.005[c]	17 ± 3[c]	600[e] ± 250	4.56[f]	0.64 ± 0.05[c]	1.14 ± 0.01

[a]The value for f/f_0 was obtained using the following equation: $\frac{f}{f_0} = \frac{\Delta F + F_0}{F_0}$. Error ranges on these values were calculated using standard propagation of errors. [b]The first row is based upon the conventional analysis. The second row (shaded) is based from the individual fits to the data by simulation. [c]Error ranges were calculated from FitSpace analysis of the individual fit by simulation with a threshold of 5% deviation from the minimal SSE. [d]Due to the rapid equilibrium (<1.3 ms) between bromide ion and the αY60W mutant of CaaD, the data only defines the K_d for bromide binding to free *E*. This k_{on} affords the calculation of the defined K_d when the k_{off} is assumed to be 200 s^{-1}. [e]This value was calculated by dividing k_{off} / k_{on}. [f]These values were held fixed during the fit by simulation. [g]K_d is calculated by dividing k_{off} / k_{on} using the values from the conventional analysis of the binding of **4** to αY60W-CaaD in a stopped-flow experiment (Figure S6A). [h]K_d is calculated from the conventional analysis of the saturation of the fluorescence signal in the stopped-flow experiment monitoring the binding of **4** to αY60W-CaaD (Figure S6B).

Table S3. Kinetic Rates Obtained from Conventional Analysis of Stopped-flow and Rapid Quench Data Using **9.**[a]

Enzyme	K_1[b] ($\mu M^{-1}s^{-1}$)	k_2[c] (s^{-1})	k_3[b] (s^{-1})	k_4[b] (s^{-1})
Wild-type	720	90	3	6
αY60W-CaaD	400	86	8	2.5
αM7W-CaaD	7500	-	12	1

[a]Rate constants are defined in Scheme 4. [b]Results from fit shown in Figure 2 (raw data shown in Figure 3B). Fit for αM7W-CaaD not shown (raw data shown in Figure S1B). [c]Value from the burst rate shown in Figure 5.

Table S4. Rates Constants Derived from the Alternate Global Analysis of the αY60W-CaaD Reaction with **9.**[a]

Rate	Lower Limit	Upper Limit	% Range	Best fit	Rate	Lower Limit	Upper Limit	% Range	Best fit
f/f_0	0.16	0.23	17%	0.2	k_3	2.4	4.0	20%	3.4 s^{-1}
					k_4	6.5	11.4	27%	9.2 s^{-1}
k_{-1}[b]	2600	4700	32%	3300 s^{-1}	$K_{d,\ Br}$[b]	9100	20000	43%	12500 μM
k_2[b]	65	100	22%	78 s^{-1}	k_{-6}[b]	20	33	26%	25 M^{-1} s^{-1}

[a]The data are fit globally to the mechanism shown in Scheme 3. [b]Rate constants and errors for k_{-1}, k_2, $K_{d,Br}$, and k_{-6} are identical to the values presented in Table 4. See Table 4 and text for more information regarding the global fit.

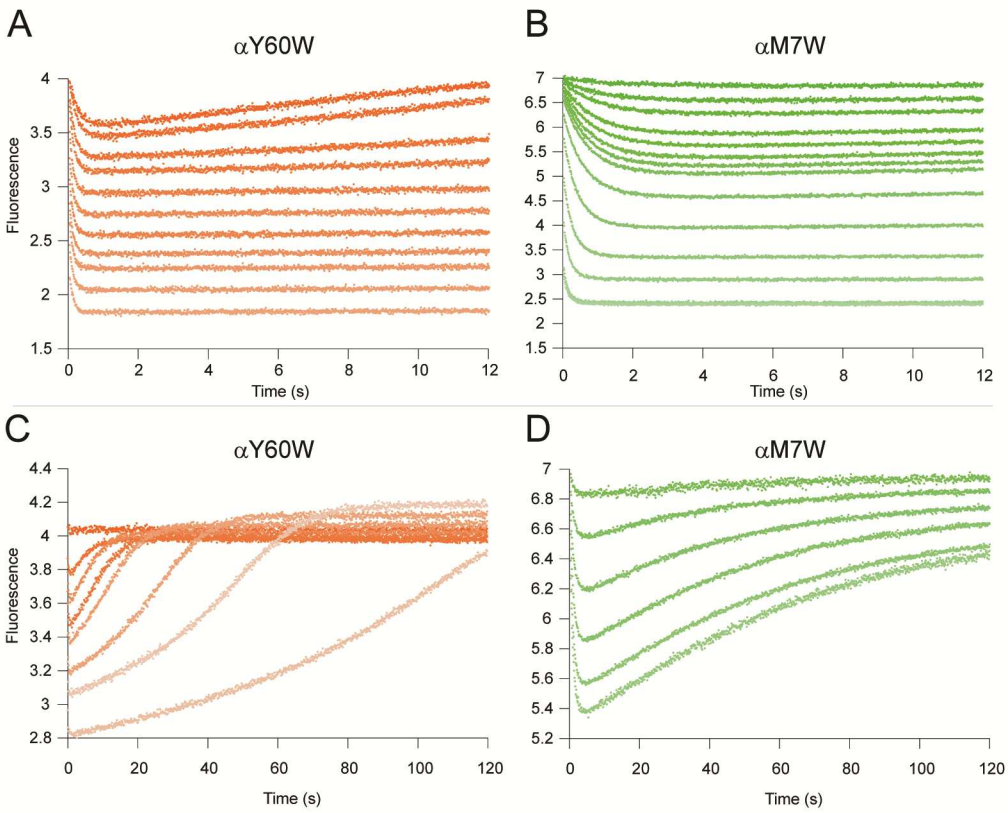

Figure S1. Stopped-flow fluorescence traces following A) αY60W-CaaD for 12 s; B) αM7W-CaaD for 12 s; C) αY60W-CaaD for 120 s; and D) αM7W-CaaD for 120 s. The αY60W-CaaD mutant shows about a 2-fold decrease in fluorescence, whereas the αM7W-CaaD mutant shows a 3.5-fold decrease over the first 1 s of the reaction. Note the smaller overall amplitude observed with αY60W-CaaD.

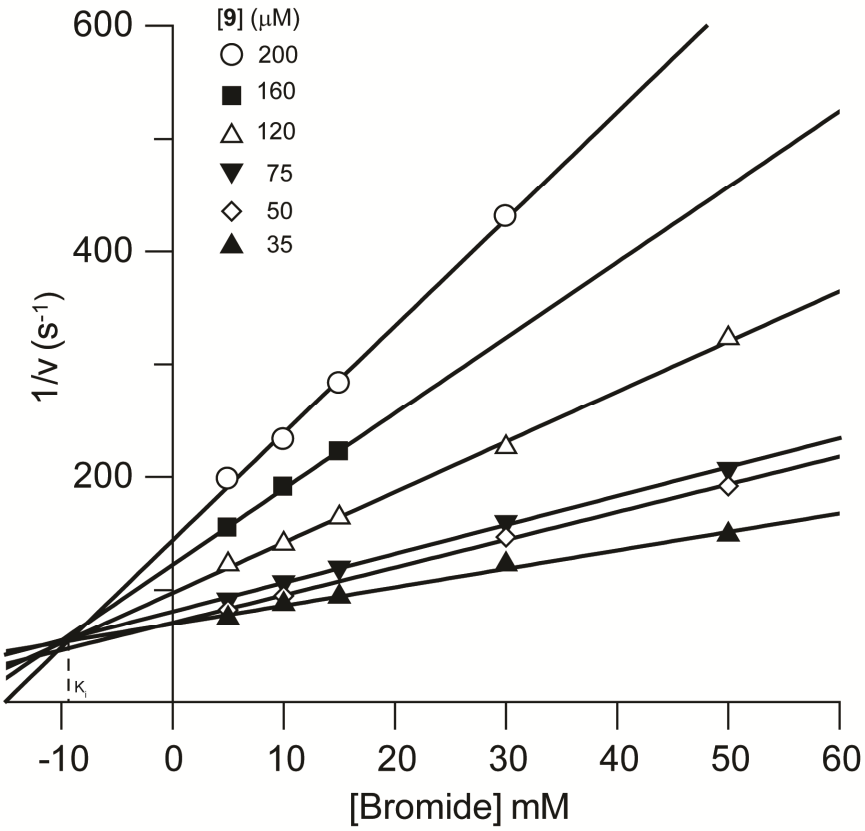

Figure S2. A Dixon plot of the initial reciprocal velocities (1/v) against bromide (5, 10, 15, 30 and 50 mM) at six concentrations of **9** (35, 50, 75, 120, 160, and 200 μM).[2] The K_i for inhibiton of αY60W-CaaD by bromide is determined by the intersection point of the lines resulting from a linear fit to the data (shown above as solid lines). The K_i of bromide (dashed lined extrapolation) was determined to be ~ 10 mM.

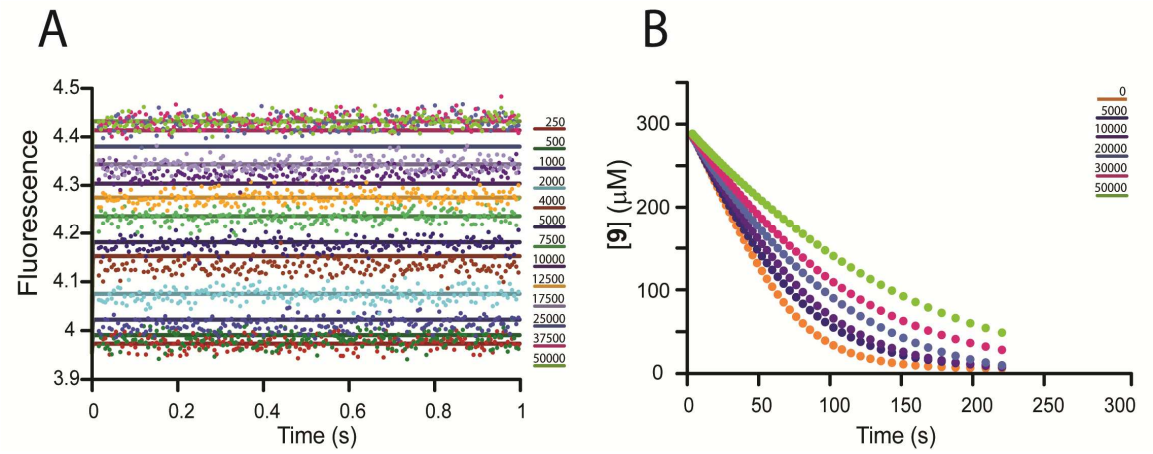

Figure S3. Bromide binding and inhibition. A) The stopped-flow fluorescence traces (340 nm) of αY60W-CaaD with bromide (0-37500 μM) over 1 s. Each trace was fit to a line (slope=0) and resulting constant values (C) were further analyzed as shown in Figure S4. Solid lines correspond to the fit by simulation. Results of the fit by simulation can be found in Table S2. B) Full progress curve kinetic traces observed at 300 μM of **9** with αY60W-CaaD in the presence of five concentrations of bromide (0, 5, 10, 20, 30, and 50 mM) are shown.

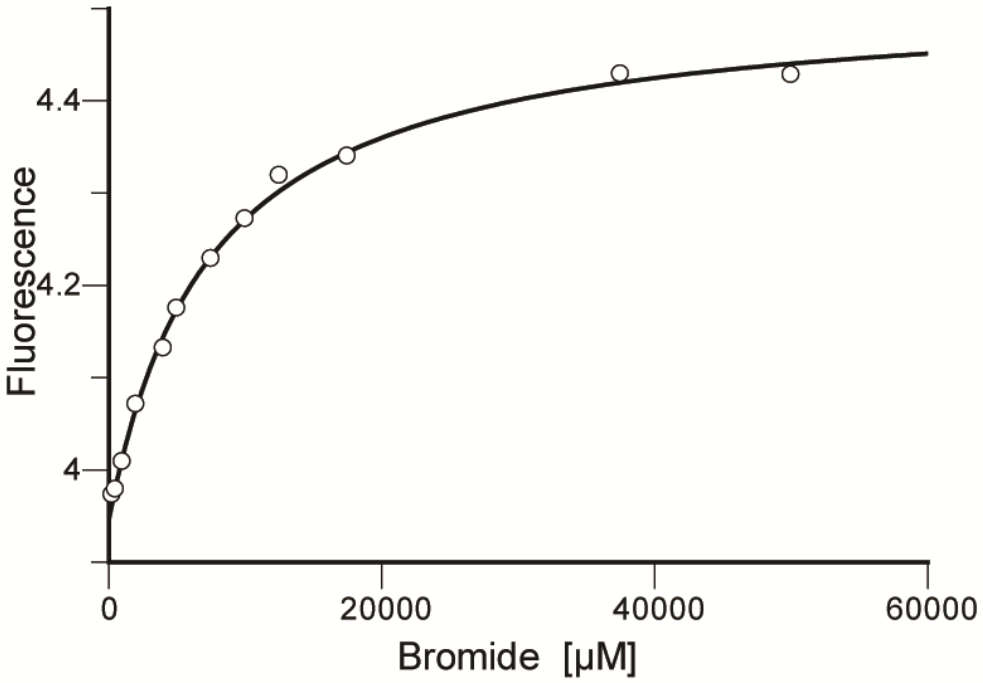

Figure S4. Bromide ion binding to the αY60W-CaaD mutant. Plot of constant values (C) vs. bromide concentration with fit (solid line) to eq S1.

$$F = F_0 + \Delta F\left(\frac{[X]}{K_D + [X]}\right) \qquad \text{(eq. S1)}$$

A summary of the fitting results is found in Table S2.

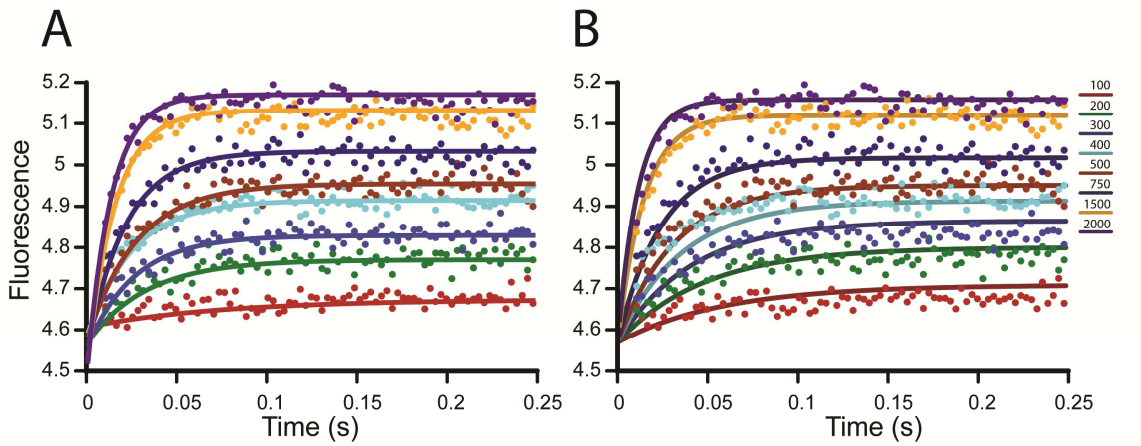

Figure S5. The stopped-flow fluorescence traces (250 ms) of αY60W-CaaD with **4** (0-2000 μM). A) Solid lines represent a single exponential fit to the data. Resultant rate vs. concentration plots are shown in Figure S6. B) Solid lines represent the fit to the data by simulation. Rate constant values resulting from the fit by simulation are found in Table S2.

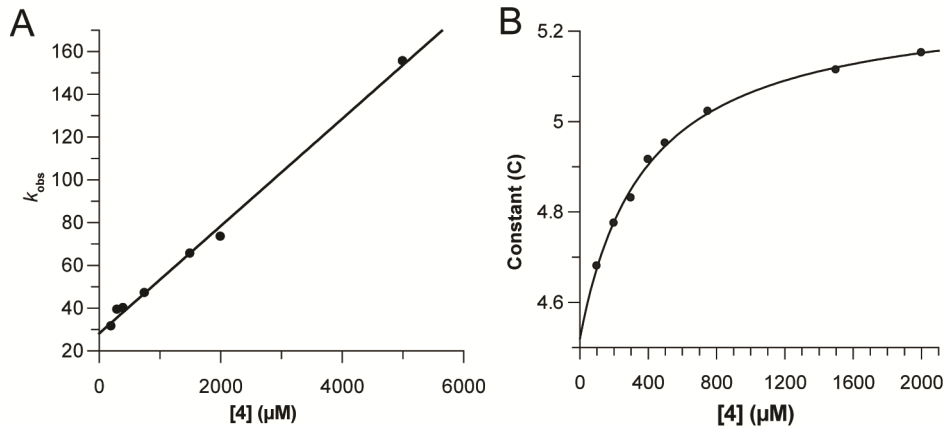

Figure S6. Conventional analysis of the binding of **4** to the αY60W-CaaD mutant.[3] A) Plot of the k_{obs} vs. [**4**] with fit to eq S2 (solid line). B) Plot of constant values (C) vs. [**4]** with fit to eq S1 (solid line).

$$k_{obs} = k_1[\mathbf{4}] + k_{-1} \qquad \textbf{Eq S2}$$

A summary of fitting results can be found in Table S2.

Text S1. The global fitting model shown in Scheme 4 incorporates two assumptions (shown in gray) regarding product release: 1) malonate semialdehyde (*Q* in Scheme 4) release from $E^{*}PQ$ is largely irreversible, and 2) binding of *P* to $E^{**}Q$ is too weak or too slow to generate $E^{*}PQ$. Although these assumptions may appear to violate the law of microscopic reversibility, their validity can be demonstrated in the product release model shown in Scheme 5.

Scheme 5

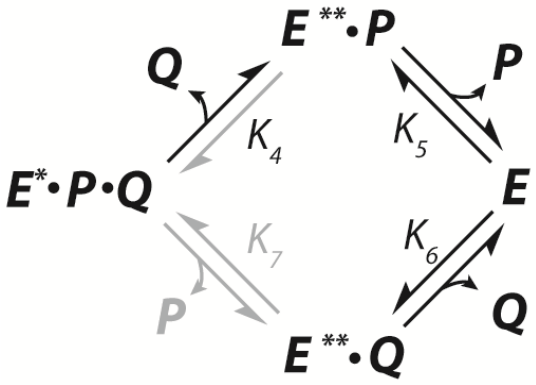

In Scheme 5, K_4 is the dissociation constant for release of *Q* from $E^{*}PQ$, K_5 is the dissociation constant for release of *P* from $E^{**}Q$, K_6 is the dissociation constant for release of *Q* from $E^{**}P$, and K_7 is the dissociation constant for release of *P* from $E^{*}PQ$. The product of all equilibrium constants contained in a thermodynamic cycle must be equal to unity. Therefore, the product of constants on one side of the pathway must be equal to the product of the constants on the other side (eq. S3):

$$K_4^D \bullet K_5^D = K_6^D \bullet K_7^D \qquad \textbf{eq S3}$$

Rearrangement of eq. S3 to make the binding of *Q* to $E^{**}P$ versus *E* equal to the binding of *P* to $E^{**}Q$ versus *E* gives eq. S4:

$$\frac{K_4^D}{K_6^D} = \frac{K_7^D}{K_5^D} \qquad \textbf{eq S4}$$

Experimental data provides approximations of the values for K_6^D (~0.6 mM) and K_5^D (~12 mM^{-1}). Substituting these values in their respective positions and rearranging yields eq S5:

$$\frac{K_4^D}{0.6} = \frac{K_7^D}{12} \qquad \textbf{eq S5}$$

Solving Eq. S5 yields eq. S6:

$$K_4^D = 20 \bullet K_7^D \qquad \textbf{eq S6}$$

Eq. S5 demonstrates that the dissociation constants for K_4^D and K_7^D are proportional. As a result, an assumption of irreversible release of **4** (large value K_4^D) would correspond to an even larger dissociation constant for Br (i.e., bromide doesn't bind to $E^{**}Q$).

Moreover, Eq. S6 shows that Q binds to species $E^{**}P$ (K_4^D) approximately 20 times tighter than P binds to species $E^{**}Q$ (K_7^D). In conclusion, the assumptions associated with the product release and rebinding in Scheme 3 are consistent with the collected data.

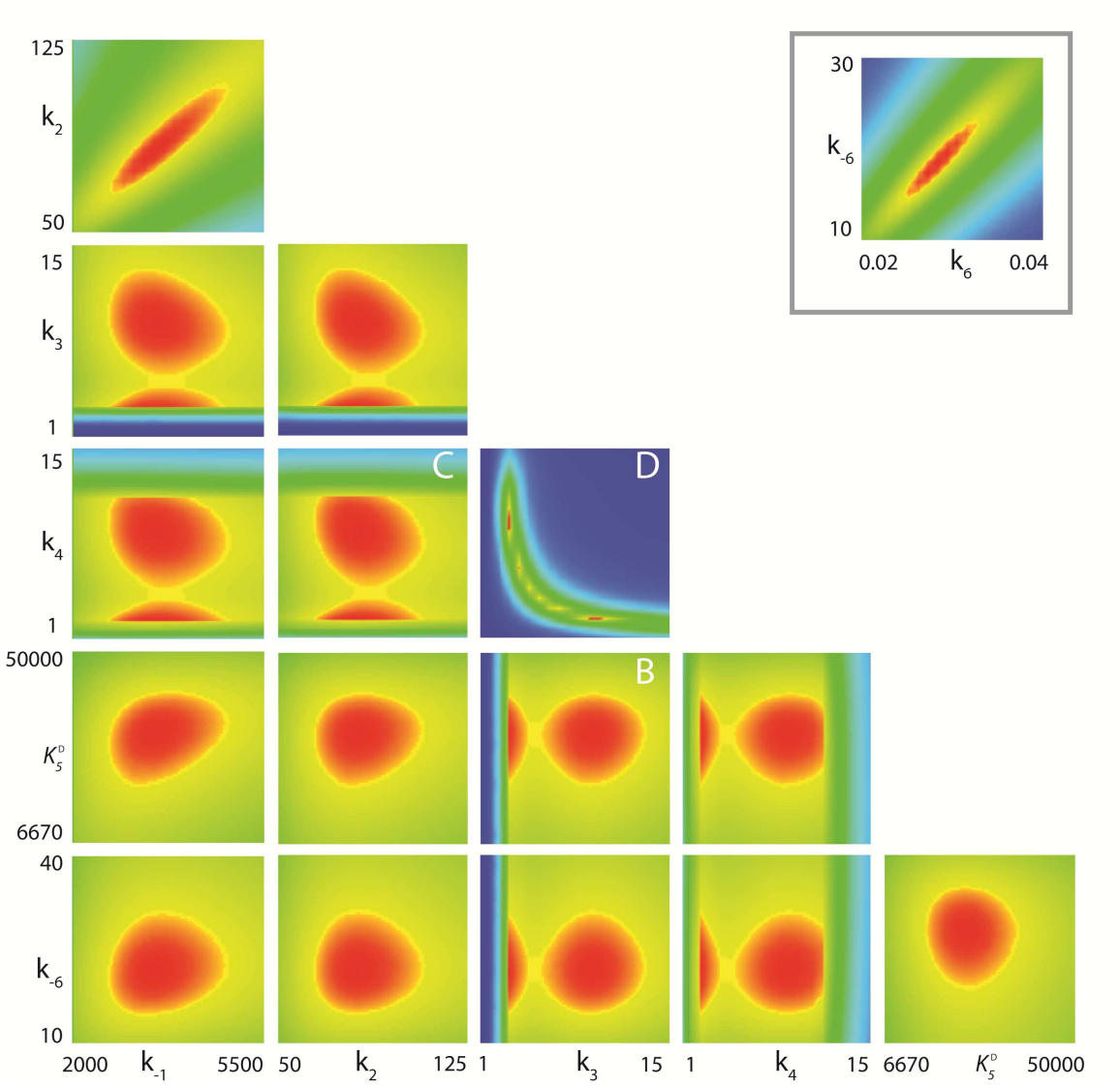

Figure S7. FitSpace confidence contours for the global fit of the kinetic data shown in Figure 7A-I (Y60W-CaaD and **9**) to the model in Scheme 4.[5] The inset shows the FitSpace confidence contours for the fit by simulation of **4** binding to αY60W-CaaD (Figure 7G). The fluorescence factor of E^{**} was held fixed at 1.13. The letters B, C, and D (shown in white) refer to select results used in Figure 8.

References:

(1) Trott, O., and Olson, A. J. (2009) AutoDock vina: improving the speed and accuracy of docking with a new scoring function, efficient optimization, and multithreading, *J. Comput. Chem.*, 455-461.

(2) Dixon, M. (1953) Determination of enzyme-inhibitor constants, *Biochem. J. 55*, 170-171.

(3) Johnson, K. A. (1992) Transient-state kinetic analysis of enzyme reaction pathways, In *The Enzymes* (Sigman, D. S., Eds.) (3rd ed.) ed., pp 1-61.

(4) Segel, I. H. (1993) *Enzyme kinetics: behavior and analysis of rapid equilibrium and steady-state enzyme systems*, Wiley Classics Library, New York.

(5) Johnson, K. A., Simpson, Z. B., and Blom, T. (2009) FitSpace explorer: an algorithm to evaluate multidimensional parameter space in fitting kinetic data, *Anal. Biochem. 387*, 30-41.